The Astrophysical Journal, 917:2 (10pp), 2021 August 10 https://doi.org/10.3847/1538-4357/ac05ba

Do the Periodic Activities of Repeating Fast Radio Bursts Represent the Spins of Neutron Stars?

Kun Xu[1,2], Qiao-Chu Li[3,4], Yuan-Pei Yang[5], Xiang-Dong Li[3,4], Zi-Gao Dai[3,4], and Jifeng Liu[1,2,6]
[1] School of Astronomy and Space Sciences, University of Chinese Academy of Sciences, Beijing, People's Republic of China; xukun@smail.nju.edu.cn
[2] Key Laboratory of Optical Astronomy, National Astronomical Observatories, Chinese Academy of Sciences, Beijing, People's Republic of China
[3] Department of Astronomy, Nanjing University, Nanjing 210023, People's Republic of China
[4] Key Laboratory of Modern Astronomy and Astrophysics, Nanjing University, Ministry of Education, Nanjing 210023, People's Republic of China
[5] South-Western Institute for Astronomy Research, Yunnan University, Kunming 650500, People's Republic of China
[6] WHU-NAOC Joint Center for Astronomy, Wuhan University, Wuhan, People's Republic of China
Received 2020 December 14; revised 2021 May 25; accepted 2021 May 25; published 2021 August 6

Abstract

Fast radio bursts (FRBs) are mysterious radio transients with millisecond durations. Recently, ∼16 days of periodic activity and ∼159 days of possible periodicity were detected to arise from FRB 180916.J0158+65 and FRB 121102, respectively, and the spin period of a slow-rotation magnetar was further considered to be one of the possible explanations of the periodic activities of repeating FRBs. For isolated neutron stars, the spin evolution suggests that it has difficulty reaching several hours. In this work, we mainly focus on the possible maximum spin period of isolated NSs/magnetars dominated by an interaction between a star's magnetic field and the disk. We find that the disk wind plays an important role in spin evolution, whose influence varies the power-law index in the evolution equation of mass flow rate. For a magnetar without disk wind, the longest spin period is tens of hours. When the disk wind with a classical parameter is involved, the maximum spin period can reach hundreds of hours. But for an extremely large index of mass flow rate due to disk wind or other angular momentum extraction processes, a spin period of ∼(16–160) days is still possible.

Unified Astronomy Thesaurus concepts: Accretion (14); Stellar accretion disks (1579); Magnetars (992); Radio bursts (1339); Stellar rotation (1629)

1. Introduction

Fast radio bursts (FRBs) are radio transients with millisecond durations and extremely high brightness temperatures. To date, hundreds of FRBs have been discovered[7] (e.g., Lorimer et al. 2007; Thornton et al. 2013; Spitler et al. 2016; Chatterjee et al. 2017; Bannister et al. 2019; Prochaska et al. 2019; Ravi et al. 2019; Marcote et al. 2020), and dozens of them are repeating sources. Although a Galactic FRB (FRB 200428; Bochenek et al. 2020; CHIME/FRB Collaboration et al. 2020b) was recently detected from a magnetar SGR J1935+2154 associated with a X-ray burst (Mereghetti et al. 2020; Li et al. 2021; Ridnaia et al. 2021; Tavani et al. 2021) during its active phase, the physical origin of FRBs is still poorly known (e.g., Katz 2018a; Cordes & Chatterjee 2019; Petroff et al. 2019; Platts et al. 2019). Based on the distance of the emission region from the neutron star (NS), various models can be divided into "close-in" models and "far-away" models. The "close-in" models proposed that FRBs are emitted from the magnetosphere of an NS due to internal triggers (e.g., Kumar et al. 2017; Lyutikov 2017; Katz 2018b; Lu & Kumar 2018; Yang & Zhang 2018; Wadiasingh & Timokhin 2019; Kumar & Bošnjak 2020; Lu et al. 2020; Lyubarsky 2020; Lyutikov & Popov 2020; Wadiasingh et al. 2020; Wang 2020; Wang et al. 2020; Yang et al. 2020) or external triggers (Zhang 2017; Dai 2020; Geng et al. 2020). And the "far-away" models suggested that FRBs are produced by a synchrotron maser in a shocked outflow (Lyubarsky 2014; Waxman 2017; Metzger et al. 2019; Beloborodov 2020; Marcote et al. 2020; Wu et al. 2020; Xiao & Dai 2020; Yu et al. 2021).

Remarkably, periodic activity of 16.35 ± 0.18 days was recently detected to arise from FRB 180916.J0158+65 (hereafter FRB 180916), and the activity window during each period is about 5 days (Chime/Frb Collaboration et al. 2020a). Very recently, with all detections of FRB 180916 from 110 to 1765 MHz (Aggarwal et al. 2020; Chime/Frb Collaboration et al. 2020a; Marthi et al. 2020; Pastor-Marazuela et al. 2020; Sand et al. 2020), the period is confirmed to be $16.29^{+0.15}_{-0.17}$ days and the activity window peaks earlier at higher frequencies (Pastor-Marazuela et al. 2020). Furthermore, the first repeating FRB, FRB 121102, also appears to have tentative periodic activity of ∼160 days (Cruces et al. 2020; Rajwade et al. 2020). Three possibilities were widely considered to explain the periodic activities of these sources (see the review of Zhang 2020): (1) the FRB source is in a binary system containing an NS, and the observed period corresponds to the orbital period of the binary system (Dai & Zhong 2020; Gu et al. 2020; Ioka & Zhang 2020; Lyutikov et al. 2020; Deng et al. 2021; Kuerban et al. 2021; Sridhar et al. 2021); (2) radio bursts are generated from a deformed NS with a narrow beam, the observed periodic activity is due to the precession like a gyroscope (Levin et al. 2020; Tong et al. 2020; Yang & Zou 2020; Zanazzi & Lai 2020; Li & Zanazzi 2021; Sridhar et al. 2021); (3) the observed period corresponds to the extremely slow rotation of an NS (Beniamini et al. 2020). Katz (2021) proposed that the modulation period may help to distinguish these models. The last possibility might be the simplest and most intriguing. If such a long period is due to the

[7] See Petroff et al. (2016) for a catalog of published FRBs (http://frbcat.org/) and the Transient Name Server system (https://www.wis-tns.org/) for newly reported FRBs (Petroff & Yaron 2020).

spin of an NS, one may have more opportunities to study the NS evolution (e.g., Xu & Li 2019) or constrain the fundamental physics (e.g., Yang & Zhang 2017). In this work, we will focus on the discussion of the last possibility, which equivalently raises a question: what is the longest possible spin period of an isolated NS?

In general, the long period of an NS could be due to magnetic dipole radiation or a supernova fallback disk.[8] The former will extract the rotational energy via the magnetic dipole radiation and let the NS lose angular momentum. In the latter case, the material in the fallback disk will be expelled if the disk is in propeller state, which will carry away the angular momentum of the NS. In this work, we mainly focus on the possible maximum spin period of isolated NSs/magnetars. Although some different mechanisms, like the winds or bursts/outbursts from magnetars (Beniamini et al. 2020; Tong & Huang 2020), may relax certain parameter requirements, a general and detailed discussion about the most likely scenario, purely fallback, is still necessary, especially for the discussion about the mysterious period of FRBs.

The pulsar 1E 161348−5055 (hereafter 1E 1613), which has a spin period of about 6.67 hr (De Luca et al. 2006), is the slowest isolated NS known by now. To explain the extreme spin period of 1E 1613, previous studies show that an ultrastrong magnetic field of $\gtrsim 10^{15}$ G is not sufficient. Extra spin-down torque is also required, which is possibly delivered by a fallback disk (De Luca et al. 2006; Li 2007; Tong et al. 2016; Ho & Andersson 2017). Xu & Li (2019; hereafter XL19) show that the initial disk mass can only be in a very small range $\sim 10^{-7}\ M_{\odot}$. Based on the model in XL19, we perform more general Monte Carlo simulations to get the longest spin period of an isolated NS interacting with a fallback disk. Furthermore, we take disk wind into account and discuss its influence. We obtain the maximum spin period of an isolated NS as ∼63 hr without considering disk wind and ∼13.5 days with a classical parameter of disk wind. While with an extremely large parameter, which is the power-law index of the mass flow rate due to disk wind or another angular momentum extraction process, we can obtain a spin period of longer than 16 days or even 160 days.

This paper is organized as follows. We discuss the period constraints of an NS, particularly the fallback disk model, in Section 2 and exhibit the results in Section 3. We discuss the range of disk wind parameter in Section 4 and summarize the paper in Section 5.

2. Mechanisms Dominating Spin Evolution of Isolated NSs

For an isolated NS without a fallback disk, the magnetic dipole radiation gives a torque $N_{\rm B} = -2\mu^2\Omega^3/3c^3$ on the NS, which leads to the spin evolution of

$$P_{\rm dip} = \left(P_{\rm i}^2 + \frac{16\pi^2}{3c^3 I}\mu^2 t\right)^{1/2} \approx 248\ {\rm s}\cdot B_{16} t_4^{1/2}, \quad (1)$$

where $P_{\rm i}$, I, and $\mu = BR_{\rm NS}^3$ are the initial spin period, moment of inertia, and magnetic dipole moment of the NS, respectively. And t_4 is the age of the NS in units of 10^4 yr. We assume that the magnetic dipole radiation is exerted on the NS in its lifetime. Consequently, we can get the maximum spin period $P_{\rm dip,max} \lesssim 248$ s for a magnetar with $B \lesssim 10^{16}$ G and $t \lesssim 10$ kyr if FRBs are from active magnetars.

As for the period of a magnetar that can generate FRBs, Wadiasingh et al. (2020) recently predicted a death line for magnetars in the framework of a low-twist magnetar magnetosphere with dislocations of magnetic footpoints inducing accelerating gaps. When the density of the charge produced by the star motion to screen the electric field is insufficient, the intense particle acceleration is produced. And the death line satisfies $P_{\rm low\text{-}twist} \gtrsim 6\ {\rm ms}\cdot B_{16}^{-1}$, which gives a lower limit of period that can generate FRBs from a magnetar. If $P_{\rm dip} > P_{\rm low\text{-}twist}$, it is possible for the magnetar to produce FRBs.

In conclusion, the longest period of an isolated NS/magnetar with the age <10 kyr cannot exceed several hundred seconds. However, since the material in the fallback disk could be expelled by the rotating magnetosphere if the disk is in propeller state, the NS could further spin down, leading to a longer period. Meanwhile, the mass transfer in the accretion process might trigger FRBs, which are generated by coherent curvature radiation of the electrons because of accretion material moving along the NS magnetic field lines (e.g., Geng et al. 2020; Gu et al. 2020). In the following, we will focus on the period constraint from the fallback disk model.

In order to better understand the periodicity of isolated NSs, especially the long period, the fallback disk model is considered. A fallback disk may form around an NS if the angular momentum of the fallback material, which is gravitationally captured after the supernova explosion, is sufficient (e.g., Wang et al. 2006). Then the disk evolves following the self-similar solutions of the viscous diffusion equation (Pringle 1981; Cannizzo et al. 1990). We use the same model in Xu & Li (2019), where the mass flow rate $\dot{m}$ (in units of Eddington accretion rate $\dot{M}_{\rm Edd}$) in the disk varies as (Liu & Li 2015)

$$\dot{m} = \dot{m}_0 (t/t_{\rm f})^{-a}. \quad (2)$$

Here $\dot{m}_0 = \dot{M}_0/\dot{M}_{\rm Edd}$ is the initial mass flow rate and $t_{\rm f}$ is the formation time of the fallback disk. The power-law index a depends on opacity and disk wind loss in the slim disk phase,

1. $a = 19/16$ for opacity dominated by electron scattering and $a = 1.25$ for Kramers opacity (Cannizzo et al. 1990; Francischelli et al. 2002; Li 2007; Tong et al. 2016).
2. $a = 4/3$ in the case without disk wind, while $a > 4/3$ on the contrary. In general, $a = 5/3$ for the strongest wind loss so that $4/3 < a < 5/3$ if the loss is weak (Pringle 1991; Cannizzo & Gehrels 2009; Shen & Matzner 2012; Liu & Li 2015; Lin et al. 2021).

In this work, we mainly discuss the influence of disk wind.

With the mass flow rate decreasing and the size expanding, the disk usually starts at a slim or thick disk phase, then translates to a thin disk and ends at a advection-dominated accretion flow (Liu & Li 2015; Xu & Li 2019). With the intention of studying the interaction between the fallback disk and the NS, we define three radii. First, the inner radius of the disk is $R_{\rm in} = \xi R_{\rm A}$, where $\xi = 1$ in this paper, and $R_{\rm A}$ is the traditional Alfvén radius for spherical accretion

$$R_{\rm A} = \left(\frac{\mu^4}{2GM_{\rm NS}\dot{M}_{\rm in}^2}\right)^{1/7}, \quad (3)$$

where G is the gravitational constant and $\dot{M}_{\rm in}$ is the mass flow rate at the inner edge of the disk. The second is the corotation

[8] In addition, gravitational wave emission (Gittins & Andersson 2019) and neutrino radiation can also lead to an NS spinning down, but their influences are too small to be considered, especially in slow spin systems.

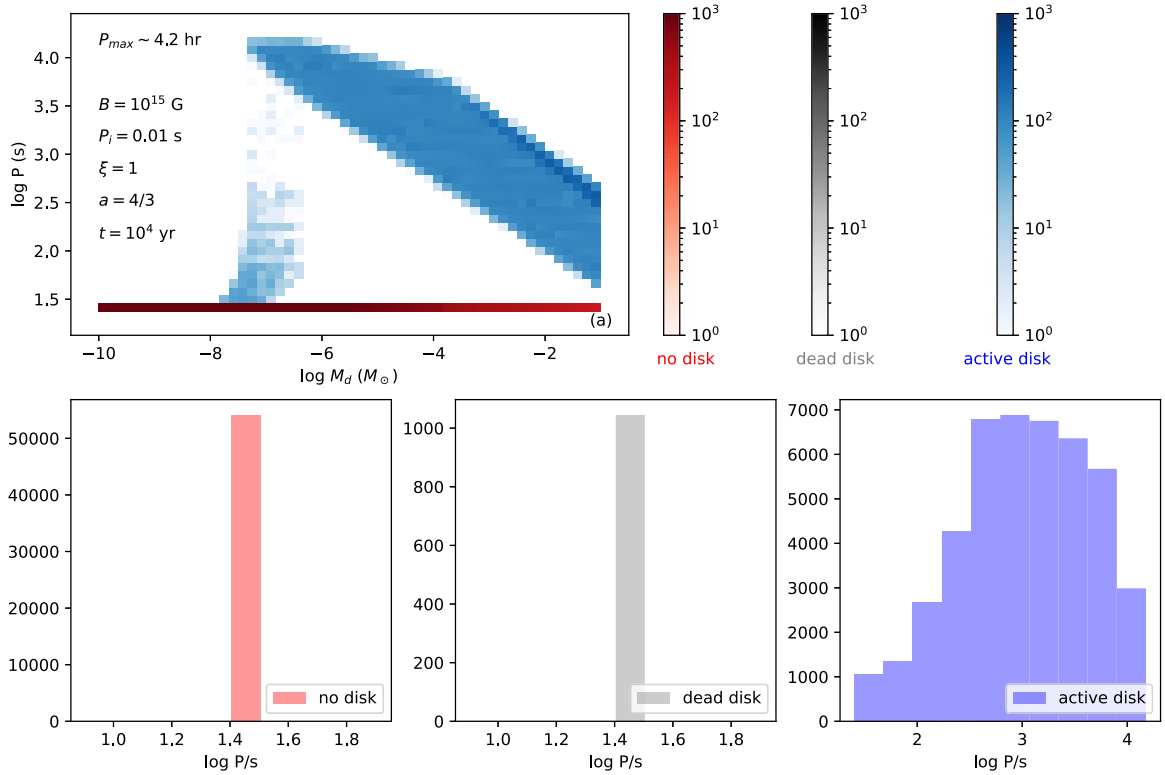

Figure 1. Top panel: distribution of spin period at an age of 10^4 yr against M_d with the magnetic field B taken to be 10^{15} G. The blue and gray colors demonstrate the cases in which the disks are in active and dead states, respectively, while the red colors mean that the disk cannot form. The color depth describes the number of NSs in each bin, which is indicated in the color bar. And the color bars are shared in all the figures of MC results in this paper if there is no color bar exhibited beside the panels. Lower panels: histograms of no disk cases, dead disk cases, and active disk cases from left to right.

radius R_c in which the Keplerian angular velocity $\Omega_K(R)$ of the disk equals the angular velocity Ω_s of the NS

$$R_c = \left(\frac{GM_{NS}}{\Omega_s}\right)^{1/3}. \quad (4)$$

Lastly, the light cylinder radius is defined as where the corotation velocity is equivalent to the speed of light c

$$R_{lc} = \frac{c}{\Omega_s}. \quad (5)$$

When $R_{in} < R_c$, accretion occurs and the NS gains angular momentum at a rate

$$N_{spin\text{-}up} = \dot{M}_{acc}(GM_{NS}R_{in})^{1/2}, \quad (6)$$

to spin up, where $\dot{M}_{acc}$ is the accretion rate onto the NS. While $R_c < R_{in} < R_{lc}$, the propeller phase is triggered and the material in the inner edge of the disk is ejected, so the NS spins down with a torque

$$N_{spin\text{-}down} = -\dot{M}_{in}(GM_{NS}R_{in})^{1/2}. \quad (7)$$

When $R_{in} > R_{lc}$, there is no interaction between the disk and the NS, and only the magnetic dipole radiation operates.

3. Results

3.1. Model without Disk Wind

We first set up $a = 4/3$ in our Monte Carlo simulation without considering disk wind. In each case, the torque supported by the fallback disk comes into operation at t_f and ends at the age of a magnetar (taken to be 10^4 or 10^5 yr in this paper) or when the disk enters the "dead disk" state where there is no interaction between the NS and the disk (Xu & Li 2019). The initial mass M_d and the outer radius R_f) of the disk are randomly distributed in the range of $[10^{-10}, 10^{-1}]$ $M_\odot$ and $[R_{NS}, 10^6 R_S]$, where $R_{NS} = 10^6$ cm and $R_S \approx 4 \times 10^5$ cm are the radius and the Schwartzschild radius of a 1.4 $M_\odot$ NS. And in each sample we simulate the evolution of 10^6 NSs. Top panel of Figure 1 shows the distribution of the spin periods P at 10^4 yr versus the initial disk mass $10^{-10}M_\odot \leqslant M_d \leqslant 10^{-1}M_\odot$.[9] Other parameters are listed in the figure, which are the magnetic field of the NS $B = 10^{15}$ G, the initial spin period of the NS $P_i = 0.01$ s, and the correction factor of the inner disk radius $\xi = 1$. The maximum spin period P_{max} is about 4.2 hr. The blue and gray colors demonstrate the cases in which the disks are in active and dead states, respectively, while the red colors mean that the disk cannot form. The color depth describes the number of NSs in each bin, which is indicated in the color bar. And the color bars are shared in all the figures of MC results in this paper if there is no color bar exhibited beside the panels. The lower panels show the histograms of no disk cases, dead disk cases, and active disk cases from left to right, respectively. Then we show the results of six groups of MC simulations with $a = 4/3$ in Figure 2. From top to bottom panels, the magnetic fields are $B = 10^{14}$, 10^{15}, and 10^{16} G, respectively. This shows that P_{max} becomes larger for stronger B, which is consistent the results in XL19. This implies that the

[9] Another free parameter is the initial outer radius of the fallback disk R_f, but the distribution of the spin periods is not very sensitive to it as shown in the left panel of Figure 2 in XL19, so we will not exhibit the results versus R_f in this paper.

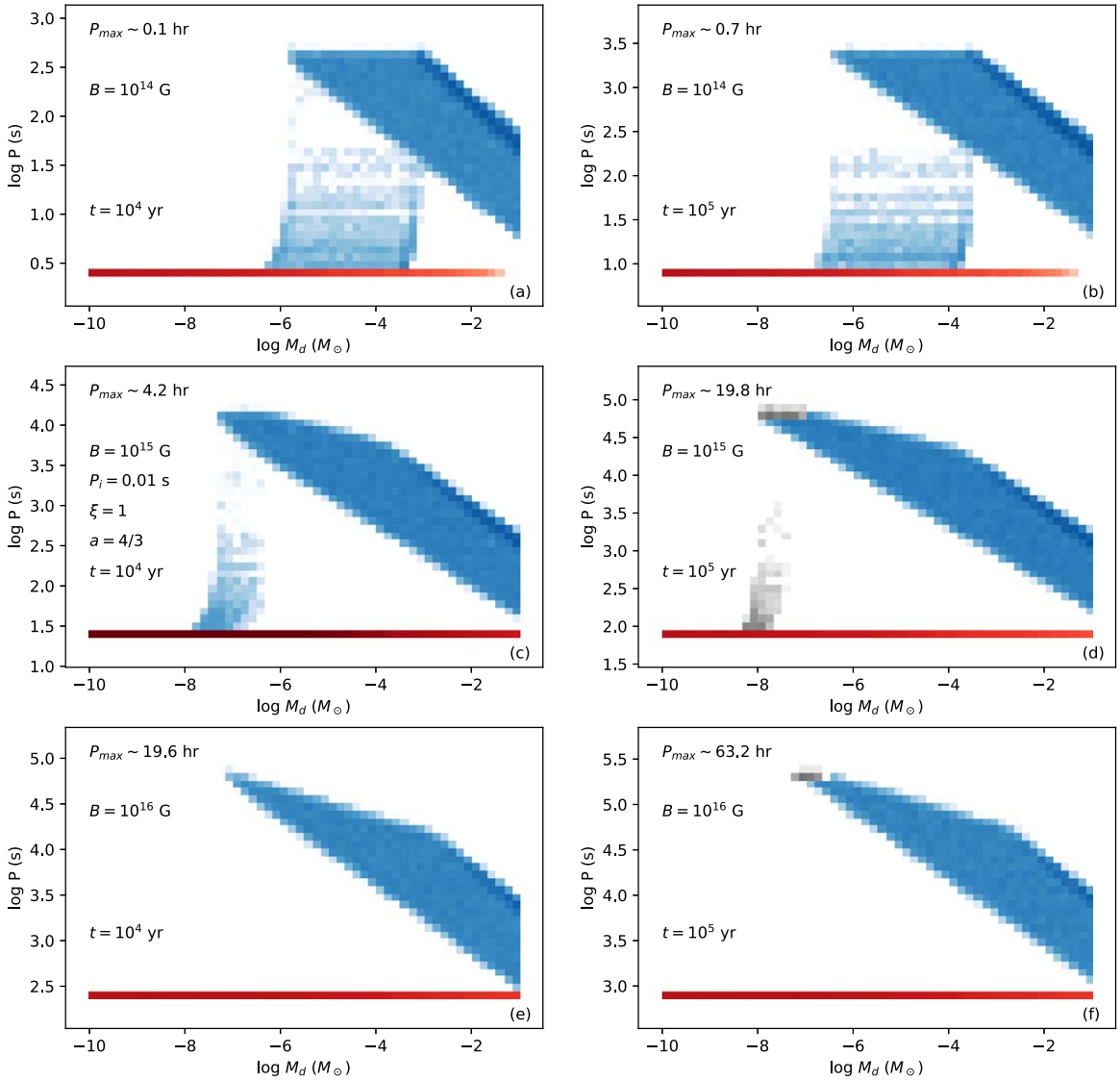

Figure 2. Distribution of spin period against $M_{\rm d}$ in six groups of MC simulations with $a = 4/3$.

NS has reached the equilibrium spin period

$$P_{\rm eq} = 2^{11/14}\pi(GM)^{-5/7}\xi^{3/2}\mu^{6/7}\dot{M}_{\rm in}^{-3/7}. \quad (8)$$

The ages of the systems are 10^4 yr in the left panels and 10^5 yr in the right panels. NSs spin down to much longer spin periods at 10^5 yr but the disks evolve to dead state in more systems.

We do more simulations with $10^{14}\,{\rm G} \leqslant B \leqslant 10^{16}\,{\rm G}$ and pick out $P_{\rm max}$ in each MC simulation group drawing in Figure 3. The filled and unfilled circles correspond to cases with $t = 10^4$ yr and 10^5 yr, respectively. The colors indicate the magnetic fields of the NS, which are demonstrated in the legend. The figure shows that $P_{\rm max} \approx 19.6$ hr at 10^4 yr and $P_{\rm max} \approx 63.2$ hr at 10^5 yr in the model without disk wind when $B = 10^{16}$ G.

3.2. Model with Disk Wind

We vary the value of a to be $5/3$ in this section to see how the disk wind can influence the spin evolution of the NS. The results are shown in Figures 4 and 5. They show that the NS can spin down to a much longer spin period under the action of disk wind. And the maximum values are also obtained when $B = 10^{16}$ G, which is $P_{\rm max} \approx 65$ hr at 10^4 yr and $P_{\rm max} \approx 325$ hr ($\approx$13.5 days) at 10^5 yr.

4. Discussion

4.1. Range of the Power-law Index a

There has been some debate regarding the value of a in the disk wind model. Beniamini et al. (2020) suggest that $a = \frac{28(p+1)}{3(7+2p)}$ and $0 \leqslant p \leqslant 1$ (Blandford & Begelman 1999) for the classical thin disk model and that it is possibly associated with radiatively inefficient accretion flows (RIAFs). In fact the rotation of the disk is thought to be sub-Keplerian when the inner region of the disk becomes RIAFs (slim/thick disk; Dall'Osso et al. 2016; Xu & Li 2017; Gao & Li 2021), so the relationship between the inner disk radius and the mass transfer rate should be $R_{\rm in} \propto \dot{M}_{\rm in}^{-1/7}$ (Dall'Osso et al. 2016) or even of a more complex form (Xu & Li 2017), rather than $R_{\rm in} \propto \dot{M}_{\rm in}^{-2/7}$. And based on the deduction process in Beniamini et al. (2020) one can get $a = \frac{28(p+1)}{3(7+p)}$ for the slim or thick disk model. When

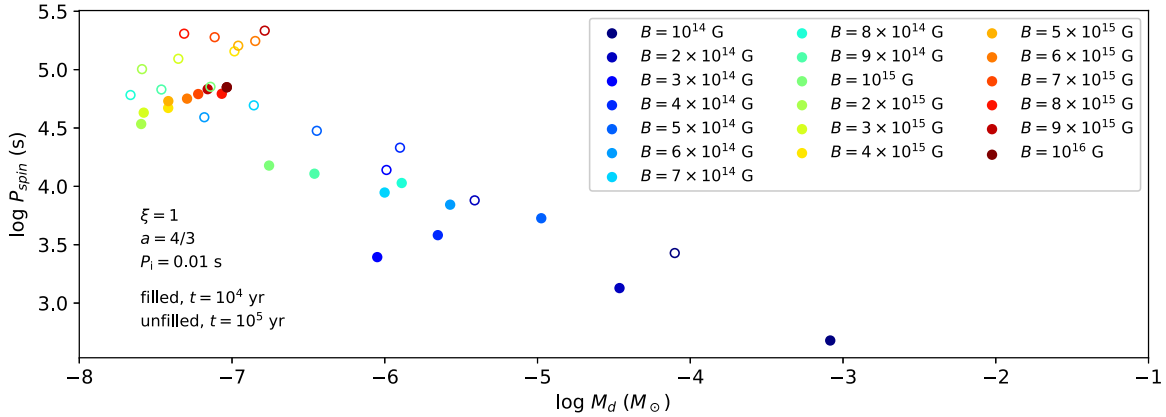

Figure 3. The maximum spin periods against M_d in the model without disk wind ($a = 4/3$). The filled and unfilled circles correspond to the case with $t = 10^4$ and 10^5 yr. The colors indicate the magnetic fields of the NS.

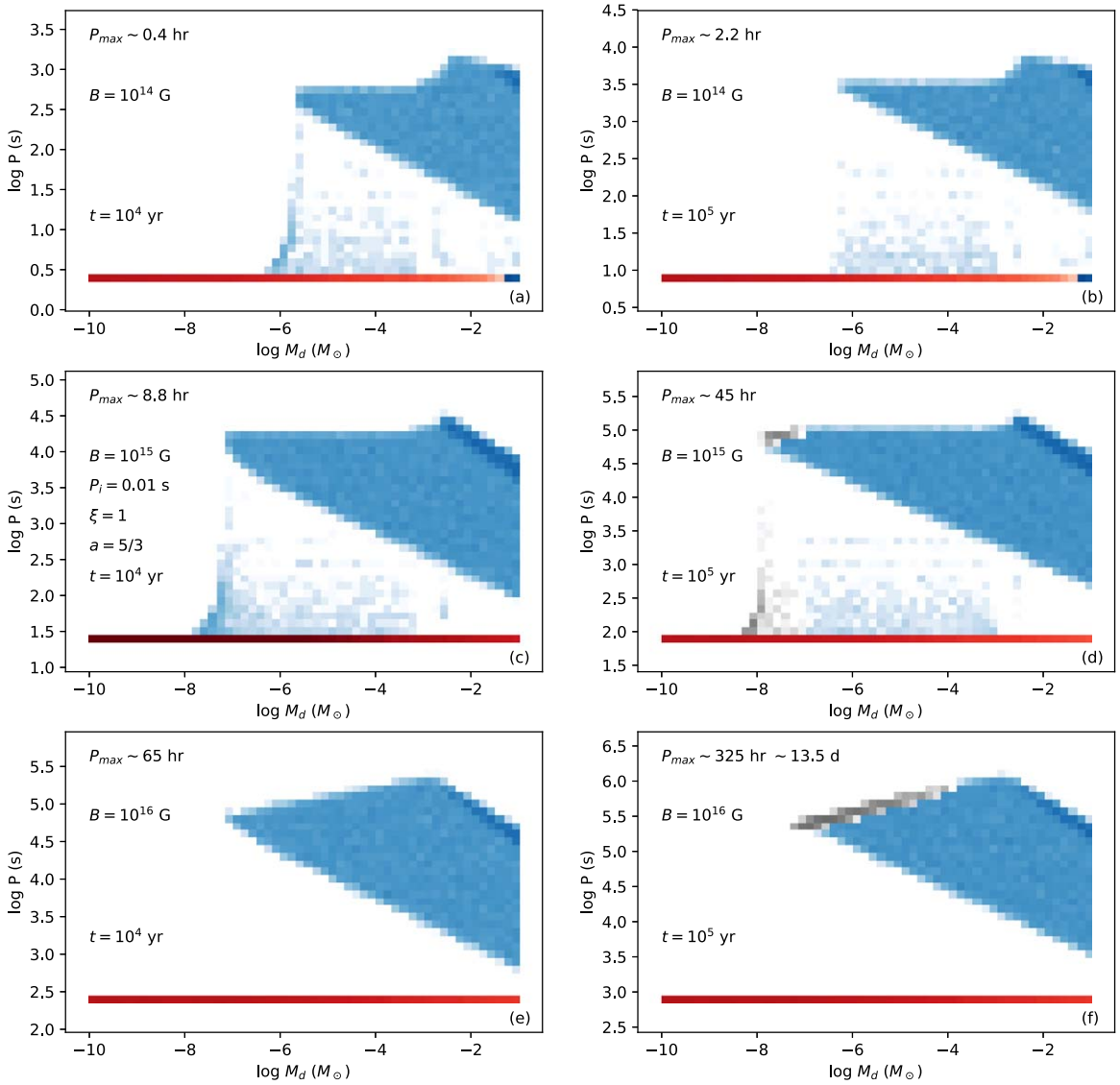

Figure 4. Same as Figure 2 but with $a = 5/3$.

$p = 0$, there is no wind (Blandford & Begelman 1999) and $0 < p \leqslant 1$ corresponding to the disk wind case, i.e., $4/3 \leqslant a \leqslant 7/3$. Combining Equations (2) and (8) we have $P_{\rm eq} \propto \dot{M}^{-3/7} \propto t^{3a/7}$. We show some cases of spin evolution path with $a = 4/3$, $5/3$, 2, and $7/3$ in Figure 6. In each curve the dashed and solid parts indicate the evolutionary stages before and after the fallback disk formed, respectively. The four curves coincide before $t \sim 10$ yr, where the disk has not

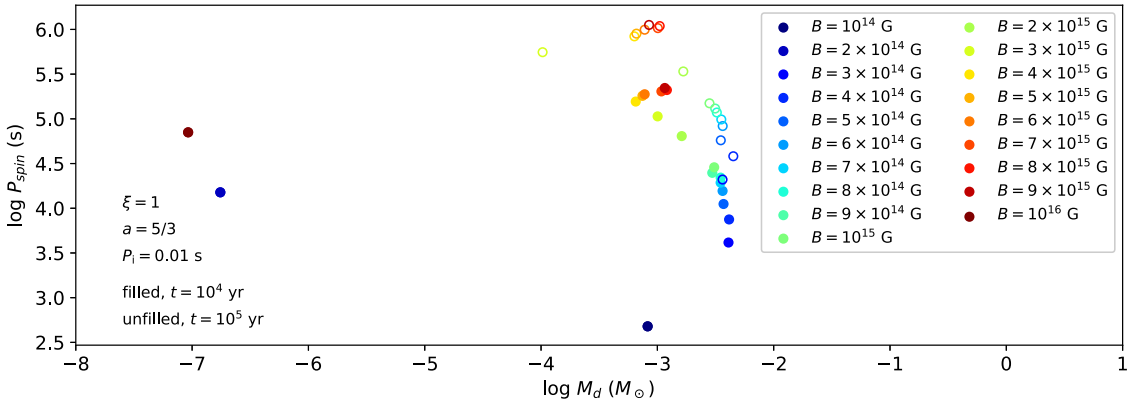

Figure 5. Same as Figure 3 but with $a = 5/3$.

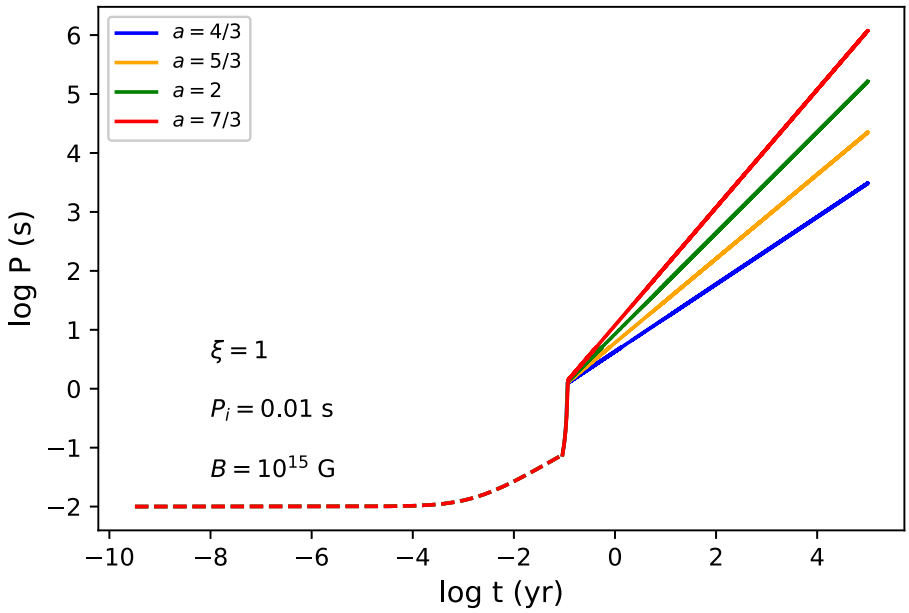

Figure 6. Spin evolution with the power-law index a taken to be 4/3, 5/3, 2, and 7/3. In all cases $M_d = 10^{-3}\ M_\odot$ and $R_f = 10^4 R_S$. The four curves coincide before $t \sim 10$ yr, where the disk has not formed (the dashed part) or is in the propeller phase (the solid part). When entering equilibrium state, the curves separate and P_{eq} becomes larger as a increases.

formed or is in the propeller phase. When entering equilibrium state, the curves separate and P_{eq} becomes larger as a increases.

"Disk winds" are thought to be observed in four NS systems, which are Her X-1 (Kosec et al. 2020; Nixon & Pringle 2020), GX 13+1 (Ueda et al. 2004), IGR J17480-2446 (Miller et al. 2011), and IGR J17591-2342 (Nowak et al. 2019). In the first three systems, outflows are probably from the inner disk in the super-Eddington accretion phase, which may be explained by the mass loss at the spherization radius because the Eddington-limited accretion is enabled (Shakura & Sunyaev 1973; Lipunova 1999; Grebenev 2017). Only in the fourth system, emission radii ranges from 1000 to 200,000 km, which is consistent with the disk wind scenario proposed in Emmering et al. (1992). The driving mechanism and energy budget of the disk wind are still not clear. The hard X-ray radiation and magnetic fields on the disk are the favored explanations (Blandford & Payne 1982; Drew & Proga 2000) in non-magnetic accretor systems, i.e., black holes, nonmagnetic cataclysmic variables, and young stellar objects. But in the NS systems, the disorganized magnetic field lines on the disk will be arranged and reconnect with the lines of the NS. So the material is possibly constrained by the reconnected lines and may have difficulty escaping from the disk.

Since $0 \leqslant p \leqslant 1$ is adapted to the disk around a black hole, which may be different in an NS system. And in observations no disk wind phenomenon was detected in isolated NS systems,[10] which may be because the fallback disk mass is too small to generate strong and sustained wind. Then from the geometrical feature, a slim disk is more likely to generate disk wind than a thin disk, but its lifetime[11] is very short, i.e., even if the disk wind were strong in the slim disk phase, it could be ignored. On the other hand, one can see from Figure 6 that an NS can easily spin down to tens of thousands of seconds within a few thousand years under the action of strong disk wind, while only one very slow isolated NS (1E 1613) was found in observation. Therefore, disk wind in isolated NS systems might be very weak, which can be ignored, and the maximum value of a is possibly not as large as 7/3, while 5/3 is more physical. So the maximum spin periods of isolated NSs are $\sim$63 hr

[10] The four NS systems thought to be observed "disk winds" are all binaries.
[11] One can see that the lifetime of a slim disk is $\lesssim$1 yr from Appendix B in XL19.

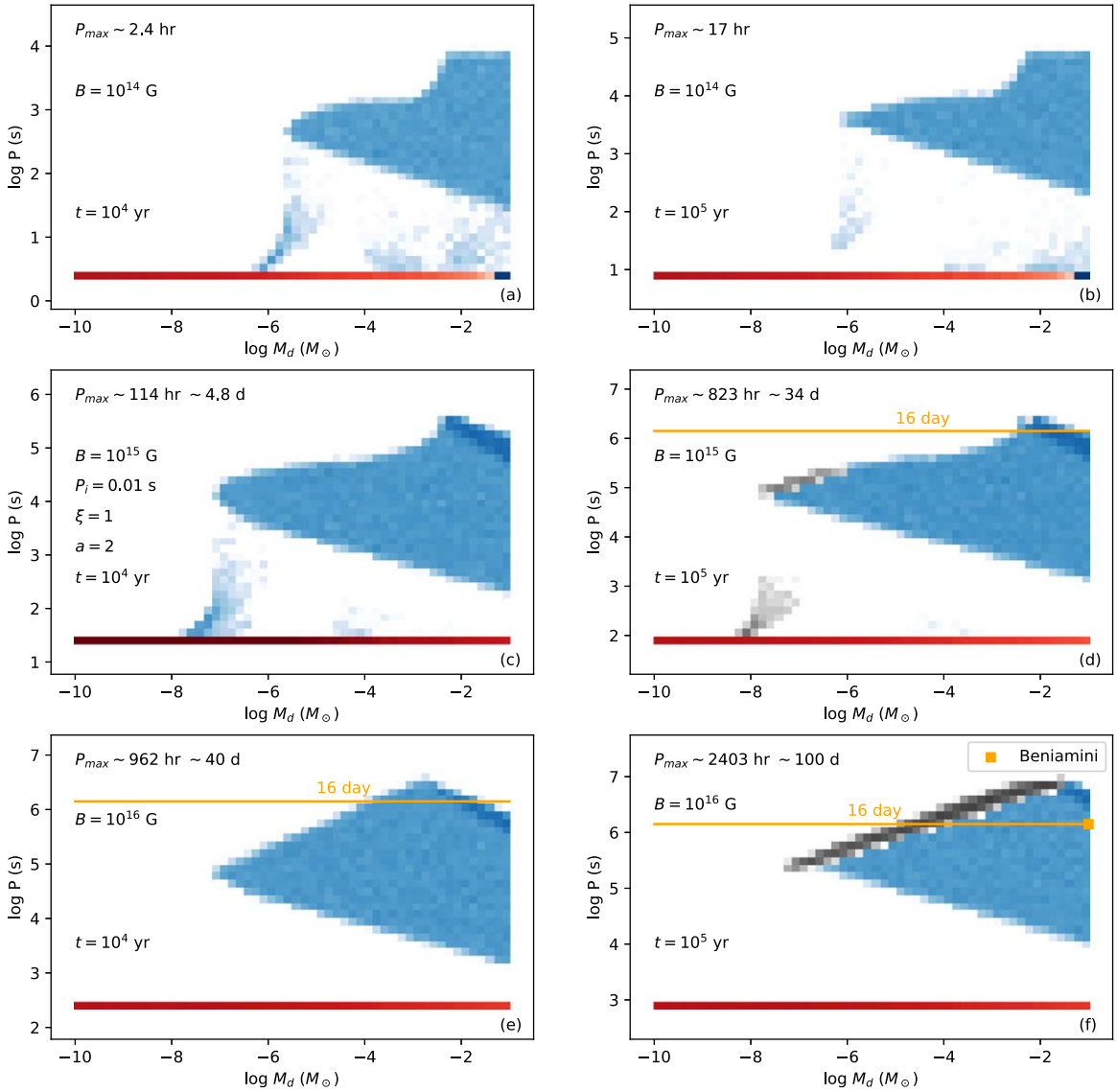

Figure 7. Same as Figure 2 with $a=2$. The orange solid line represents the spin period of 16 days. The orange square corresponds to the results in Beniamini et al. (2020).

without considering disk wind and ∼13.5 days with disk wind at 10^5 yr.

4.2. Periodicity in FRB 180916 and 121102

As shown above, the maximum spin period of an isolated NS/magnetar is ∼13.5 days with a power-law index of $a\leqslant 5/3$, which is widely acceptable and in accordance with theory and observation. Since the possibility of the ultrastrong disk wind cases with $a>5/3$ cannot be ruled out, we also do the MC simulations with $a=2$ and $a=7/3$. We show all the results of 24 groups of MC simulations in Figures 2, 4, 7, and 8 with $a=4/3$, 5/3, 2, and 7/3, respectively. The orange and green solid lines represent the spin period of 16 days and 160 days, respectively. It shows that the spin period can be larger than 16 days or even 160 days in some groups when $a>5/3$. The orange square in the lower right panel of Figure 7 corresponds to the results in Beniamini et al. (2020), which is covered by our results. The parameter spaces with $P>16$ days and $P>160$ days are exhibited in Table 1. Figure 9 displays the distribution of NS age against $M_{\rm d}$ when the spin periods reach 16 days (the left panels) and 160 days (the right panels) in the case with $a=7/3$. It shows that an NS can spin down to 16 days within a few hundred years, which is much shorter than the age of a magnetar, if the magnetic field is as extremely strong as 10^{16} G and the power-law index is as awfully large as 7/3. So if one can give a physical meaning of $a>5/3$, the long spin period of magnetars may connect to the repeating FRBs and perhaps some other interesting results of magnetars can be obtained.

If 16 days or more is indeed the period of a magnetar, it is an open question what kind of mechanism and process can produce repeating FRBs. The slowest isolated pulsar, 1E 1613, in the supernova remnant RCW 103 has a spin period of ∼6.67 hr (De Luca et al. 2006) and can be explained by a magnetar interacting with a fallback disk (Xu & Li 2019). When the fallback disk is in propeller state, the period of the magnetar will become long. Although the matter on the disk is thrown out by the centrifugal force, there is still a small part of the material that may fall into the poles of the NS along the

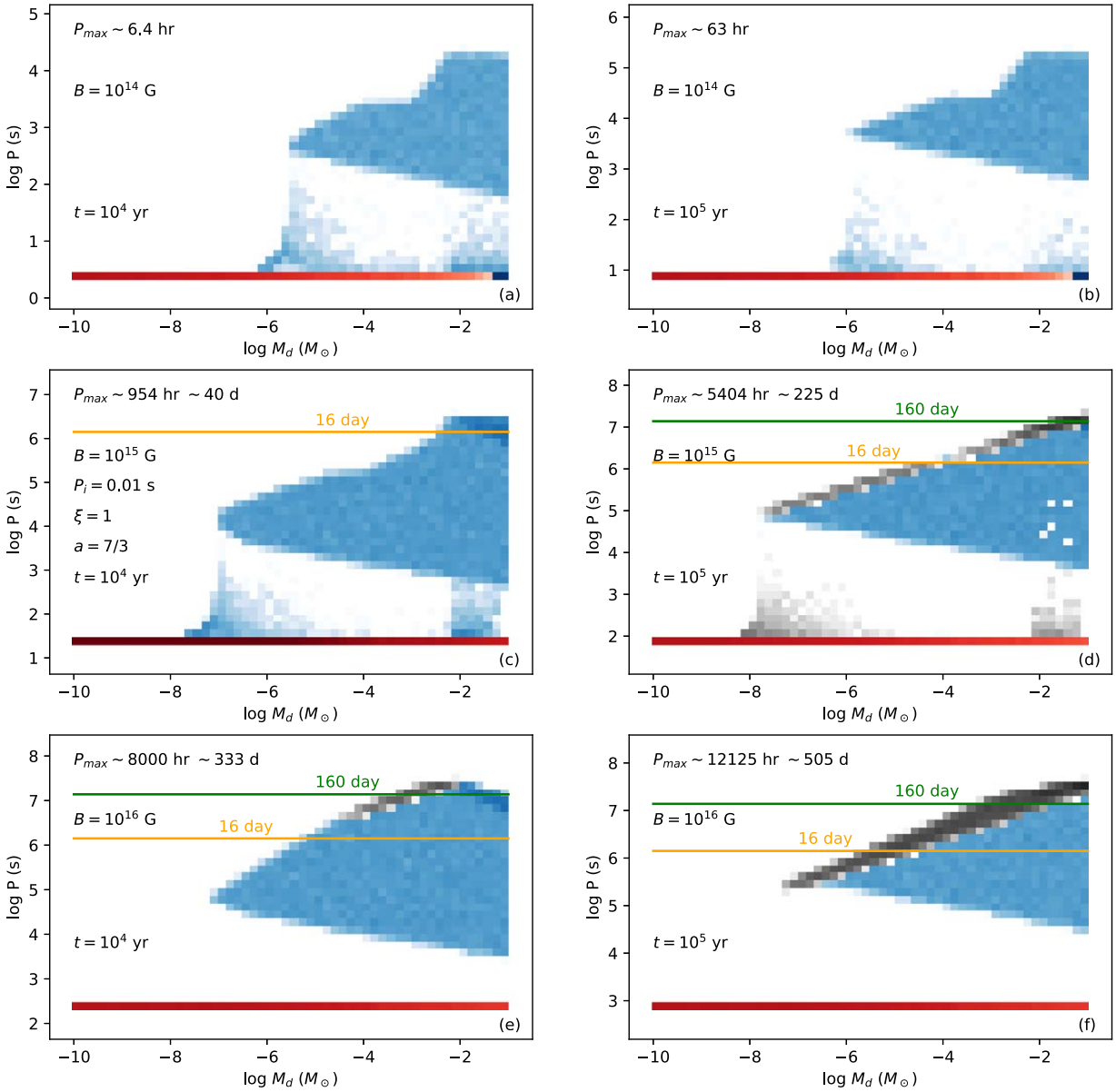

Figure 8. Same as Figure 2 with $a=7/3$. The orange and green solid lines represent the spin period of 16 days and 160 days, respectively.

Table 1
Parameter Spaces with $P>16$ days and $P>160$ days

a	B/G	t/yr	$M_d/M_\odot$ ($P>16$ days)	$M_d/M_\odot$ ($P>160$ days)
2	10^{15}	10^5	$[3\times10^{-3},\ 5\times10^{-2}]$	⋯
	10^{16}	10^4	$[2\times10^{-4},\ 2\times10^{-2}]$	⋯
		10^5	$[10^{-5},\ 10^{-1}]$	⋯
7/3	10^{15}	10^4	$[4\times10^{-3},\ 10^{-1}]$	⋯
		10^5	$[6\times10^{-5},\ 10^{-1}]$	$[2\times10^{-2},\ 10^{-1}]$
	10^{16}	10^4	$[7\times10^{-6},\ 10^{-1}]$	$[6\times10^{-4},\ 7\times10^{-2}]$
		10^5	$[2\times10^{-6},\ 10^{-1}]$	$[6\times10^{-4},\ 10^{-1}]$

magnetic field line. However, if the periodicity of an FRB is caused by the rotation of the magnetar itself, it may be more possible for short period magnetars with a more effective accretion. This process of producing FRBs is similar to an impact between an asteroid and a magnetar because of accretion (Geng et al. 2020).

5. Summary

The periods of some repeating FRBs, FRB 180916 and FRB 121102, may be from a binary system, the precession, or the spin of an NS.[12] In this work, we explore the possibly longest spin period of an isolated NS interacting with a fallback disk with and without disk wind to explain the periodic activity of FRB 180916. Our results show that $P_{\rm max}\sim 63$ hr without considering disk wind ($a=4/3$) and $P_{\rm max}\sim 13.5$ days with a classical parameter of disk wind ($4/3<a\leqslant 5/4$) if the magnetic field of the NS is as extremely strong as 10^{16} G and does not decay within 10^5 yr. However, we can obtain the spin period of hundreds of days with a large index of mass flow rate. Yet the following arguments suggest that such strong disk wind ($a>5/3$) around a highly magnetic NS may be unphysical:

[12] The binary scenario seems disfavored by Pastor-Marazuela et al. (2020) and the simplest precession models seem inconsistent with polarization measurements (Nimmo et al. 2021).

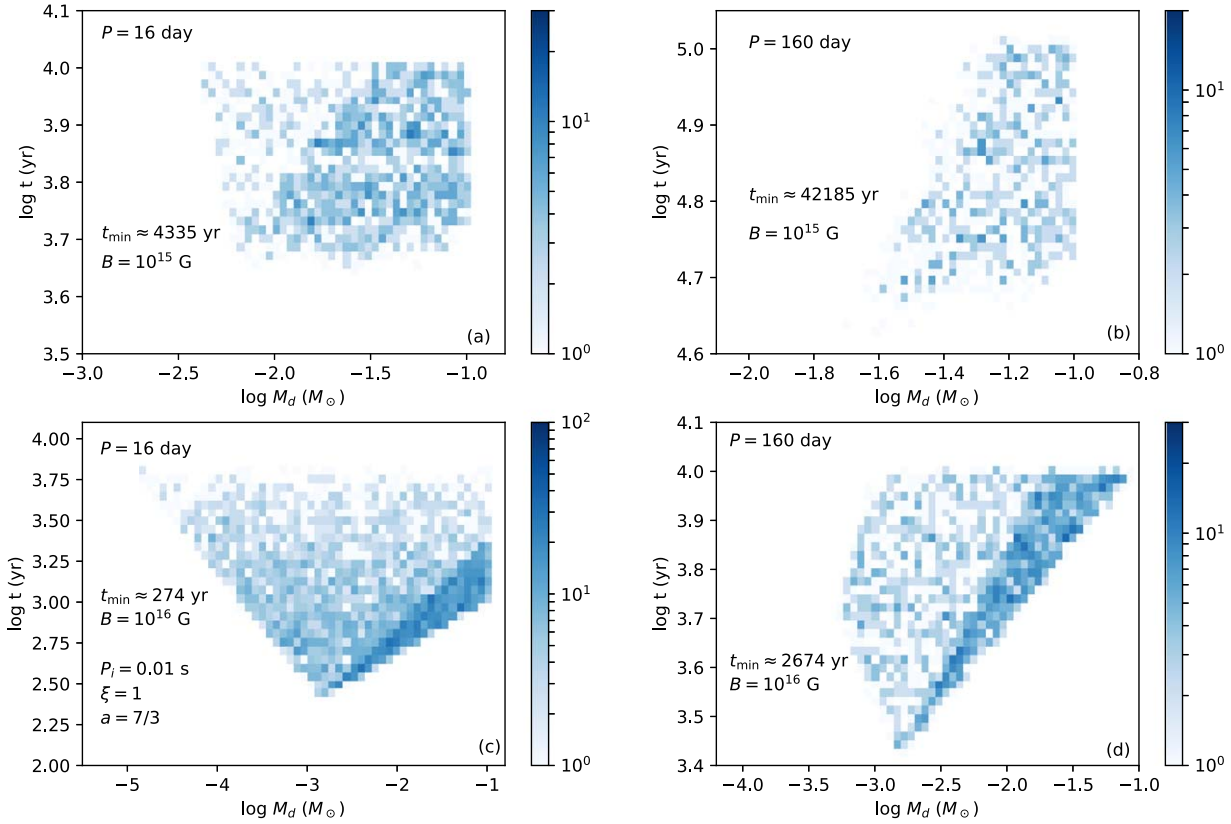

Figure 9. Distribution of NS age against $M_{\rm d}$ when the spin periods reach 16 days (the left panels) or 160 days (the right panels) in the cases with $a = 7/3$.

1. From the geometrical feature, a slim disk (or RIAF from Beniamini et al. 2020) is more likely to generate disk wind than a thin disk, but its lifetime is very short, i.e., even if the disk wind were strong in the slim disk phase, it can be ignored.
2. The fallback disk mass is usually too small ($<0.1M_{\odot}$) to generate strong and sustained wind.
3. None of disk wind phenomenon was detected in isolated NS systems.
4. The slowest isolated pulsar and accreting X-ray binary pulsar are 1E 161348+5055 with $P_{\rm spin} \approx 24{,}000$ s (De Luca et al. 2006) and AX J1910.7+0917 with $P_{\rm spin} \approx 36{,}200$ s (Sidoli et al. 2017), respectively. But they are all detected in X-ray and no radio observation is reported, which maybe indicate that they are in the "grave yard" of radio pulsars.

We find that the possible maximum spin period of an isolated NS is ∼13.5 days[13] with $a \leqslant 5/3$. Therefore, the periodic activity of these repeating FRBs may not be due to the NS spin if standard fallback disk models are invoked.

We thank the anonymous referee for helpful comments and suggestions. We thank Victoria Kaspi, Wei-Li Lin, and Xuan Fang for helpful discussions. This work was supported by the Natural Science Foundation of China under grant Nos. 11773015, 11833003, 11933004, 11988101, 12041301, and 12063001. Y.P.Y. is supported by the National Natural Science Foundation of China grant No. 12003028 and Yunnan University grant No. C176220100087.

[13] Since the slowest pulsar in isolated and binary systems known by now are both detected in X-ray, as well as considering the "grave yard" of radio pulsars, we suggest this pulsation should be in X-ray rather than radio.

ORCID iDs

Kun Xu https://orcid.org/0000-0002-9739-8929
Yuan-Pei Yang https://orcid.org/0000-0001-6374-8313
Xiang-Dong Li https://orcid.org/0000-0002-0584-8145
Zi-Gao Dai https://orcid.org/0000-0002-7835-8585

References

Aggarwal, K., Law, C. J., Burke-Spolaor, S., et al. 2020, RNAAS, 4, 94
Bannister, K. W., Deller, A. T., Phillips, C., et al. 2019, Sci, 365, 565
Beloborodov, A. M. 2020, ApJ, 896, 142
Beniamini, P., Wadiasingh, Z., & Metzger, B. D. 2020, MNRAS, 496, 3390
Blandford, R. D., & Begelman, M. C. 1999, MNRAS, 303, L1
Blandford, R. D., & Payne, D. G. 1982, MNRAS, 199, 883
Bochenek, C. D., Ravi, V., Belov, K. V., et al. 2020, Natur, 587, 59
Cannizzo, J. K., & Gehrels, N. 2009, ApJ, 700, 1047
Cannizzo, J. K., Lee, H. M., & Goodman, J. 1990, ApJ, 351, 38
Chatterjee, S., Law, C. J., Wharton, R. S., et al. 2017, Natur, 541, 58
Chime/Frb Collaboration, Amiri, M., Andersen, B. C., et al. 2020a, Natur, 582, 351
CHIME/FRB Collaboration, Andersen, B. C., Bandura, K. M., et al. 2020b, Natur, 587, 54
Cordes, J. M., & Chatterjee, S. 2019, ARA&A, 57, 417
Cruces, M., Spitler, L. G., Scholz, P., et al. 2020, MNRAS, 500, 448
Dai, Z. G. 2020, ApJL, 897, L40
Dai, Z. G., & Zhong, S. Q. 2020, ApJL, 895, L1
Dall'Osso, S., Perna, R., Papitto, A., Bozzo, E., & Stella, L. 2016, MNRAS, 457, 3076
De Luca, A., Caraveo, P. A., Mereghetti, S., Tiengo, A., & Bignami, G. F. 2006, Sci, 313, 814
Deng, C.-M., Zhong, S.-Q., & Dai, Z.-G. 2021, arXiv:2102.06796
Drew, J. E., & Proga, D. 2000, NewAR, 44, 21
Emmering, R. T., Blandford, R. D., & Shlosman, I. 1992, ApJ, 385, 460
Francischelli, G. J., Wijers, R. A. M. J., & Brown, G. E. 2002, ApJ, 565, 471
Gao, S.-J., & Li, X.-D. 2021, arXiv:2103.16068
Geng, J.-J., Li, B., Li, L.-B., et al. 2020, ApJL, 898, L55
Gittins, F., & Andersson, N. 2019, MNRAS, 488, 99

Grebenev, S. A. 2017, AstL, 43, 464
Gu, W.-M., Yi, T., & Liu, T. 2020, MNRAS, 497, 1543
Ho, W. C. G., & Andersson, N. 2017, MNRAS, 464, L65
Ioka, K., & Zhang, B. 2020, ApJL, 893, L26
Katz, J. I. 2018a, PrPNP, 103, 1
Katz, J. I. 2018b, MNRAS, 481, 2946
Katz, J. I. 2021, MNRAS, 502, 4664
Kosec, P., Fabian, A. C., Pinto, C., et al. 2020, MNRAS, 491, 3730
Kuerban, A., Huang, Y.-F., Geng, J.-J., et al. 2021, arXiv:2102.04264
Kumar, P., & Bošnjak, Ž. 2020, MNRAS, 494, 2385
Kumar, P., Lu, W., & Bhattacharya, M. 2017, MNRAS, 468, 2726
Levin, Y., Beloborodov, A. M., & Bransgrove, A. 2020, ApJL, 895, L30
Li, C. K., Lin, L., Xiong, S. L., et al. 2021, NatAs, 5, 378
Li, D., & Zanazzi, J. J. 2021, ApJL, 909, L25
Li, X.-D. 2007, ApJL, 666, L81
Lin, W., Wang, X., Wang, L., & Dai, Z. 2021, ApJL, 914, L2
Lipunova, G. V. 1999, AstL, 25, 508
Liu, B. S., & Li, X.-D. 2015, ApJ, 814, 75
Lorimer, D. R., Bailes, M., McLaughlin, M. A., et al. 2007, Sci, 318, 777
Lu, W., & Kumar, P. 2018, MNRAS, 477, 2470
Lu, W., Kumar, P., & Zhang, B. 2020, MNRAS, 498, 1397
Lyubarsky, Y. 2014, MNRAS, 442, L9
Lyubarsky, Y. 2020, ApJ, 897, 1
Lyutikov, M. 2017, ApJL, 838, L13
Lyutikov, M., Barkov, M. V., & Giannios, D. 2020, ApJL, 893, L39
Lyutikov, M., & Popov, S. 2020, arXiv:2005.05093
Marcote, B., Nimmo, K., Hessels, J. W. T., et al. 2020, Natur, 577, 190
Marthi, V. R., Gautam, T., Li, D. Z., et al. 2020, MNRAS, 499, L16
Mereghetti, S., Savchenko, V., Ferrigno, C., et al. 2020, ApJL, 898, L29
Metzger, B. D., Margalit, B., & Sironi, L. 2019, MNRAS, 485, 4091
Miller, J. M., Maitra, D., Cackett, E. M., Bhattacharyya, S., & Strohmayer, T. E. 2011, ApJL, 731, L7
Nimmo, K., Hessels, J. W. T., Keimpema, A., et al. 2021, NatAs, 5, 594
Nixon, C. J., & Pringle, J. E. 2020, A&A, 636, A34
Nowak, M. A., Paizis, A., Jaisawal, G. K., et al. 2019, ApJ, 874, 69
Pastor-Marazuela, I., Connor, L., van Leeuwen, J., et al. 2020, arXiv:2012.08348
Petroff, E., Barr, E. D., Jameson, A., et al. 2016, PASA, 33, e045
Petroff, E., Hessels, J. W. T., & Lorimer, D. R. 2019, A&ARv, 27, 4
Petroff, E., & Yaron, O. 2020, TNSAN, 160, 1
Platts, E., Weltman, A., Walters, A., et al. 2019, PhR, 821, 1
Pringle, J. E. 1981, ARA&A, 19, 137
Pringle, J. E. 1991, MNRAS, 248, 754
Prochaska, J. X., Macquart, J.-P., McQuinn, M., et al. 2019, Sci, 366, 231
Rajwade, K. M., Mickaliger, M. B., Stappers, B. W., et al. 2020, MNRAS, 495, 3551
Ravi, V., Catha, M., D'Addario, L., et al. 2019, Natur, 572, 352
Ridnaia, A., Svinkin, D., Frederiks, D., et al. 2021, NatAs, 5, 372
Sand, K. R., Gajjar, V., Pilia, M., et al. 2020, ATel, 13781
Shakura, N. I., & Sunyaev, R. A. 1973, A&A, 500, 33
Shen, R.-F., & Matzner, C. D. 2012, EPJWC, 39, 07006
Sidoli, L., Israel, G. L., Esposito, P., Rodríguez Castillo, G. A., & Postnov, K. 2017, MNRAS, 469, 3056
Spitler, L. G., Scholz, P., Hessels, J. W. T., et al. 2016, Natur, 531, 202
Sridhar, N., Metzger, B. D., Beniamini, P., et al. 2021, arXiv:2102.06138
Tavani, M., Casentini, C., Ursi, A., et al. 2021, NatAs, 5, 401
Thornton, D., Stappers, B., Bailes, M., et al. 2013, Sci, 341, 53
Tong, H., & Huang, L. 2020, MNRAS, 497, 2680
Tong, H., Wang, W., Liu, X. W., & Xu, R. X. 2016, ApJ, 833, 265
Tong, H., Wang, W., & Wang, H.-G. 2020, RAA, 20, 142
Ueda, Y., Murakami, H., Yamaoka, K., Dotani, T., & Ebisawa, K. 2004, ApJ, 609, 325
Wadiasingh, Z., Beniamini, P., Timokhin, A., et al. 2020, ApJ, 891, 82
Wadiasingh, Z., & Timokhin, A. 2019, ApJ, 879, 4
Wang, J.-S. 2020, ApJ, 900, 172
Wang, W.-Y., Xu, R., & Chen, X. 2020, ApJ, 899, 109
Wang, Z., Chakrabarty, D., & Kaplan, D. L. 2006, Natur, 440, 772
Waxman, E. 2017, ApJ, 842, 34
Wu, Q., Zhang, G. Q., Wang, F. Y., et al. 2020, ApJL, 900, L26
Xiao, D., & Dai, Z.-G. 2020, ApJL, 904, L5
Xu, K., & Li, X.-D. 2017, ApJ, 838, 98
Xu, K., & Li, X.-D. 2019, ApJ, 877, 138
Yang, H., & Zou, Y.-C. 2020, ApJL, 893, L31
Yang, Y.-P., & Zhang, B. 2017, ApJ, 842, 23
Yang, Y.-P., & Zhang, B. 2018, ApJ, 868, 31
Yang, Y.-P., Zhu, J.-P., Zhang, B., et al. 2020, ApJL, 901, L13
Yu, Y.-W., Zou, Y.-C., Dai, Z.-G., et al. 2021, MNRAS, 500, 2704
Zanazzi, J. J., & Lai, D. 2020, ApJL, 892, L15
Zhang, B. 2017, ApJL, 836, L32
Zhang, B. 2020, Natur, 582, 344